Planta
DOI 10.1007/s00425-012-1703-1

EMERGING TECHNOLOGIES

Two-photon excitation chlorophyll fluorescence lifetime imaging: a rapid and noninvasive method for in vivo assessment of cadmium toxicity in a marine diatom *Thalassiosira weissflogii*

Yan Zeng · Yun Wu · Dong Li · Wei Zheng · Wen-Xiong Wang · Jianan Y. Qu

Received: 12 May 2012 / Accepted: 24 June 2012

Abstract We demonstrate that a two-photon excitation fluorescence lifetime imaging technology can rapidly and noninvasively assess the cadmium (Cd)-induced toxic effects in a marine diatom *Thalassiosira weissflogii*. The chlorophyll, an intrinsic fluorophore, was used as a contrast agent for imaging of cellular structures and for assessment of cell toxicity. The assessment is based on an imaging-guided statistical analysis of chlorophyll fluorescence decay. This novel label-free imaging method is physically based and free of tedious preparation and preprocessing of algal samples. We first studied the chlorophyll fluorescence quenching induced by the infrared two-photon excitation laser and found that the quenching effects on the assessment of Cd toxicity could be well controlled and calibrated. In the toxicity study, chlorophyll fluorescence lifetime images were collected from the diatom samples after exposure to different concentrations of Cd. The alteration of chloroplast structure at higher Cd concentration was clearly identified. The decay of chlorophyll fluorescence extracted from recorded pixels of high signal-to-noise ratio in the fluorescence lifetime image was analyzed. The increase of average chlorophyll fluorescence lifetime following Cd treatment was observed, indicating the Cd inhibition effect on the electron transport chain in photosynthesis system. The findings of this study show that the temporal characteristics of chlorophyll fluorescence can potentially be utilized as a biomarker for indicating Cd toxicity noninvasively in algal cells.

Keywords Two-photon excitation fluorescence lifetime imaging · Chlorophyll fluorescence · Algae (*Thalassiosira weissflogii*) · Photosynthesis · Cadmium (Cd) toxicity

Abbreviations

Cd	Cadmium
PS	Photosystem
LHCII	Light-harvesting complex II
PAM	Pulse-amplitude-modulated
Φ_m	Maximum quantum yield
Φ'_m	Operational quantum yield
FLIM	Fluorescence lifetime imaging
DCMU	3-(3,4-Dichlorophenyl)-1,1-dimethyl urea
TPE	Two-photon excitation
PMT	Photo multiplier tube
TCSPC	Time-correlated single photon counting

Introduction

Toxic metals (e.g., Cd, Hg, Ni) associated with many industrial processes are significant pollutants in the aquatic environments (Bertrand and Poirier 2005). Cadmium (Cd) is one of the important toxic pollutants as it enters into the aquatic environment and is transported along the food chain. It has been reported that excessive amount of Cd released into the environment leads to retardation of plant

Y. Zeng · D. Li · W. Zheng · J. Y. Qu (✉)
Department of Electronic and Computer Engineering, Hong Kong University of Science and Technology (HKUST), Clear Water Bay, Kowloon, Hong Kong, People's Republic of China
e-mail: eequ@ust.hk

Y. Zeng
e-mail: zydrean@ust.hk

Y. Wu · W.-X. Wang
Division of Life Science, Hong Kong University of Science and Technology (HKUST), Clear Water Bay, Kowloon, Hong Kong, People's Republic of China

Published online: 18 July 2012

growth and even death due to the inhibition of various metabolic processes such as photosynthesis and respiration activities (Das et al. 1997; Bertrand and Poirier 2005; Hasan et al. 2009). To study Cd toxicity, a number of experiments performed in vitro have demonstrated that Cd interacts with Photosystem (PS), causing the structure alteration of chloroplasts (Tkalec et al. 2008), impeding the chlorophyll biosynthesis (Stobart et al. 1985; Pandey and Sharma 2002), disorganizing the light-harvesting complex II (LHCII) antenna system (Krupa 1988), and affecting the photosynthetic electron transport chain (Baszynski et al. 1980; Siedlecka and Baszynski 1993). However, the conventional in vitro analytical techniques require complicated sample preparation and processing that could not only introduce significant experimental error, but also set limitations to study or monitor the dynamic processes of the toxicity at cellular level. Therefore, an in vivo measurement method that provides noninvasive and continuous assessment of Cd-induced toxicity in the living plants during the environmental monitoring is more desirable.

Compared with the commonly used biomarkers including cell-specific growth rate, CO_2 fixation, and O_2 evolution, it has been found that the fluorescence signals could offer rather rapid and efficient detection to quantify the photosynthesis noninvasively (Maxwell and Johnson 2000; Baker 2008). Typically, a pulse-amplitude-modulated (PAM) fluorescence method was used to study the inhibition of electron transport and the variation of energy dissipation due to Cd toxicity (ElJay et al. 1997; Juneau et al. 2002). Miao et al. (2005) have demonstrated that the electron transport chain in the PSII of four types of algae was affected to different degrees by measuring the maximum quantum yield (Φ_m) and operational quantum yield (Φ'_m) utilizing PAM. However, although PAM is able to evaluate the Cd effects on plants and algae in vivo, it still requires sample preprocessing (dark adaptation) for at least 15 min following a relatively long testing period (Miao et al. 2005). Furthermore, conventional nonimaging PAM lacks the ability to show the morphological change of cells and the micrographic details of damages in chloroplast resulting from the limitation of its operational modality (Trampe et al. 2011). A number of groups have explored the fluorescence lifetime imaging (FLIM) technology to study the photosynthesis systems (Broess et al. 2009; Petrášek et al. 2009; Iwai et al. 2010). Significant increase of the average chlorophyll fluorescence lifetime was observed when the electron transport chain was blocked by the inhibitors such as 3-(3,4-Dichlorophenyl)-1,1-dimethyl urea (DCMU) (Petrášek et al. 2005; Broess et al. 2009). Recently, we used a two-photon excitation FLIM (TPE-FLIM) technique to study the toxigenicity mechanisms of inorganic mercury [Hg(II)] and methylmercury (MeHg) on photosynthesis system of a marine diatom (*Thalassiosira weissflogii*) (Wu et al. 2012). The differences in the toxigenicity mechanisms between Hg(II) and MeHg were clearly revealed with the entirely dissimilar chlorophyll fluorescence lifetime decay responses. Therefore, we hypothesize that FLIM can be potentially employed to interrogate the toxicity of Cd in algae or other plant cells by determining the changes in the temporal characteristics of chlorophyll fluorescence.

In this work, we focus to study the Cd-induced toxicity in a marine diatom *T. weissflogii* using the TPE-FLIM technique that provides a microscopic imaging and fluorescence lifetime measurements of the imaged sample simultaneously. The chlorophyll fluorescence lifetime components and average lifetime distributions are measured using the statistical and quantitative analyses of the fluorescence sectioning images of chloroplasts. Because concerns existed that excitation laser light causes chlorophyll fluorescence quenching via the state transition, singlet–singlet annihilation, proton gradient-dependent quenching (Gilmore et al. 1995; Schödel et al. 1996; Barzda et al. 2001; Szabó et al. 2005), which affects the fluorescence lifetime of chlorophyll fluorescence, we study the relationship between fluorescence lifetime components, (as well as average fluorescence lifetime distribution) and laser excitation power (Broess et al. 2009). We show that the extracted average fluorescence lifetime is a good indicator of Cd toxicity as long as the excitation is stable and controlled at safe level (Broess et al. 2009). To reduce the error in the quantitative analysis of fluorescence decay, an image-guided method is used to extract the subcellular features of high chlorophyll fluorescence signals (Li et al. 2008; Iwai et al. 2010). Finally, the DCMU-treated experiment is conducted to show that the average chlorophyll fluorescence lifetime indeed increases, resulting from inhibition of electron transport chain.

Materials and methods

Algal cultures

The diatom, *T. weissflogii* (CCMP 1587), purchased from the Provasoli-Guillard National Center of Marine Phytoplankton, was cultured in f/2 medium at 23.5 °C under an illumination of 90 μmol photons m^{-2} s^{-1} with a 14:10 h light:dark cycle. The seawater collected from 10 km off the Eastern Hong Kong shore was filtered through a 0.22-μm GP Express PLUS Membrane (Sericup, Millipore Corporation) before use. Nutrients (N, P, Si and vitamins) were passed through a Chelex 100 ion-exchange resin (Bio-Rad Laboratories) column to remove the background metals. The cells were transferred from the f/2 medium to the f/2-f/10 (trace metal level) medium for about 1-week

acclimation before the experiments under the same temperature and light conditions. All the polycarbonate beakers and bottles used in this experiment were soaked in 1 mol L^{-1} HCl and rinsed at least seven times with Milli-Q water (18.2 MΩ) before use.

Cadmium and DCMU exposure experiments

The 0.22-μm filtered and chelexed (chelex 100 ion-exchange resin) artificial seawater was used as the exposure medium (Miao et al. 2005). Similar treated nutrient stocks (N, P, Si and vitamins) were added at f/2 levels, and the trace metals were added at f/10 levels. We also used the chelating agent nitrilotriacetate (NTA, 0.1 mmol L^{-1}) and suprapure NaOH to control the free Cd ion concentration and pH (8.2 ± 0.1), respectively. The total dissolved Cd concentrations settings were 2×10^{-9} (control), 2×10^{-8}, 2×10^{-7}, 3×10^{-6}, 8×10^{-6} and 3×10^{-5} mol L^{-1}, respectively. The correspondingly free Cd ion concentration [Cd^{2+}] calculated by the MINEQL+ software for above treatments were 9.26×10^{-12}, 9.29×10^{-11}, 9.67×10^{-10}, 2.51×10^{-8}, 9.81×10^{-8}. and 4.71×10^{-7} mol L^{-1}, respectively. There were two replicates for each treatment.

After acclimation, the mid-exponential cells were then collected by centrifugation (1,800*g*, 5 min, 24 °C) and rinsed several times with artificial seawater before being inoculated to the Cd exposure medium. The initial cell density was 5×10^4 cells mL^{-1}. The total exposure experiments lasted for 72 h and were conducted under the same conditions as the algal cultures. The cell density was determined by the Coulter particle counter Z1 every 24 h. The specific growth rate was calculated from the following equation:

$$\mu = \frac{\ln c_{t_2} - \ln c_{t_1}}{t_2 - t_1}$$

where c_{t_1} and c_{t_2} were the cell density at time t_1 and t_2, respectively.

At the beginning (0 h) and the end of the experiment (72 h), 10-mL samples were concentrated to 0.5 ml by centrifugation from each replicated bottle for fluorescence lifetime analysis. During the DCMU inhibition experiment, DCMU (final concentration 10^{-5} M) was added to the mid-exponential algal cells, and after 3-h exposure, the cells were harvested by centrifugation for fluorescence analysis. DMSO was the solvent of DCMU, and the algae added with or without DMSO served as the negative controls.

Setup for measuring chlorophyll fluorescence

Fluorescence lifetime imaging was performed with a home-made two-photon FLIM system coupled to a Zeiss microscope (Zeng et al. 2011). A tunable Ti–sapphire laser (Mira 900, Coherent) pumped by Verdi (Coherent) laser was employed as the excitation source. The excitation wavelength was tuned to 850 nm, with ~150 fs pulse width and 80 MHz repetition rate. The laser beam was collimated and focused onto the sample by a water immersion objective lens [40×, 1.1 numerical aperture (NA), Zeiss]. A sampling area 75 × 75 μm^2 was created by a pair of galvo mirrors. The sectioning depth was set by manipulating an actuator (Model Z625B, Thorlabs). The tested algae were placed on the glass slides and sandwiched by a cover glass. The excited epifluorescence was separated from the excitation pulses by a dichroic mirror (760 nm, Chroma) and further purified by a short-pass filter (740 nm, Chroma) and bandpass filter (675 ± 25 nm, Chroma). The photo multiplier tube (PMT) with a time-correlated single photon counting (TCSPC) module (PML-100-20 and SPC-730, Becker & Hickl GmbH) was applied to measure the fluorescence. The integrated time was set to be 8 s for collecting each sectioning image. 200, 400, 800 μw excitation power are corresponding to the photon density: 0.215, 0.43, 0.86 mol photons m^{-2} $pulse^{-1}$ s^{-1}. It should be emphasized that the photo density in the algae cells is determined by the collimation of excitation laser beam and the optical properties of the objective lens.

Fluorescence lifetime analysis and image-guided method for pixel extraction

In this study, two replicates of *T. weissflogii* from six gradient [Cd^{2+}] concentration-treated samples were measured. Sectioning images (128 × 128 pixels with 256 time channels) were collected from each replicate and the minimum separated distance among these images was larger than 500 μm. The measurement for each replicate was completed within 30 min after sample preparation. An incomplete dual exponential fitting model, $A_1\exp(-t/\tau_1) + A_2\exp(-t/\tau_2) + A_1\exp[-(t + \Delta\tau)/\tau_1] + A_2\exp[-(t + \Delta\tau)/\tau_2]$, for fluorescence lifetime analysis, was utilized to analyze the decay curve for each image pixel after deconvolution with system response by commercial software (SPCImage, Becker & Hickle GmbH). A_1 and A_2 are the relative amplitudes of two decay terms ($A_1 + A_2 = 1$) while τ_1 and τ_2 are the lifetime components, respectively. The lifetime detecting range of the TCSPC module for each excitation pulse $\Delta\tau$ is 12.5 ns, determined by the pulse repetition rate.

The average fluorescence lifetime was calculated using the following equation: $\tau_{\text{average}} = A_1\,\tau_1 + A_2\,\tau_2$. To collect the pixels representing the sample sites of high signal-to-noise ratio and reduce the fitting errors in those pixels with few photon counts in a better way, we set a threshold equal to the half of the maximum photon counts in each measured image to reject the pixels with low photon counts

(Iwai et al. 2010). This image-guided method guaranteed that all the pixels used for analysis could provide accurate fitting results. The pixel lifetime values from each sample group images were analyzed using the dual exponential decay model. Next, we obtained the average fluorescence lifetime distribution for each [Cd^{2+}] concentration-treated samples by grouping extracted pixels from at least 4 images for each replicate.

Results

Analysis of fluorescence lifetime from extracted image pixels

The procedure to extract the pixels of high signal-to-noise ratio for fluorescence decay analysis using an image-guided method is displayed in Fig. 1. The typical gray level fluorescence intensity image is shown in Fig. 1a where gray levels represent different fluorescence intensities in each pixel from black to white. Figure 1b is the average fluorescence lifetime image scaled by intensity, while Fig. 1c shows the average chlorophyll fluorescence lifetime images without intensity scaling. The extracted imaging pixels using a threshold equal to half of the maximum counts in the picture are shown in Fig. 1d. These extracted pixels then were grouped for each replicate and used in the statistical analysis (Iwai et al. 2010).

Dependency of chlorophyll fluorescence lifetime to excitation intensity

Next, we studied the effects of excitation intensity on the chlorophyll fluorescence decay in vivo. Three different types of excitation powers at safe levels (<2 mw), which should not induce any irreversible damage to photosynthesis system, were applied in the two-photon FLIM measurements (Tirlapur and König 2001; Broess et al. 2009). The relationships between chlorophyll fluorescence lifetime distribution and laser excitation power measured from the control samples are shown in Fig. 2. The color-coded fluorescence lifetime images of *T. weissflogii* at three excitation levels are displayed in Fig. 2a–c. Indeed, a significant shift of fluorescence lifetime distribution could be observed when higher laser excitation power was employed (Fig. 2d). Specifically, the fluorescence distribution peaks were around ~980, ~760 and 580 ps, corresponding to the excitation power ~200, ~400 and ~800 μw, respectively. We observed significant decrease of lifetime components as shown in Table 1 (τ_1: 789, 662, 407 ps; τ_2: 1,594, 1,184, 1,044 ps) with increase of excitation power (~200, ~400, ~800 μw). In addition, the fluorescence excitation efficiency drops with increase of excitation power. For example, excitation efficiency at 800 μw is about fivefold less in comparison with that at 200 μw excitation. The results indicate that the precise control and stabilization of excitation power is crucial when any information extracted from the fluorescence decay is used for in vivo assessment of a biological process in *T. weissflogii.*

Analysis of Cd toxicity

In the toxicity study, the cell-specific growth rates, one of commonly used biomarkers was first used to evaluate the Cd toxicity (Das et al. 1997; Pandey and Sharma 2002; Bertrand and Poirier 2005; Miao et al. 2005; Hasan et al. 2009). The growth rate under different [Cd^{2+}] concentrations treated for *T. weissflogii* are shown in Fig. 3. A gentle decrement was observed in the first three treatments with lower [Cd^{2+}] concentrations, while a significant decrease started when the [Cd^{2+}] reached a threshold level of ~2.51×10^{-8} M. Figure 4a displays the average fluorescence lifetime image of *T. weissflogii* control samples at 0 h, while Fig. 4b–g shows the images under different [Cd^{2+}] concentrations after 72 h of exposure. The data were calculated from the FLIM measurements with the excitation power at 800 μw. Clear chloroplast degradation could be observed in the highest [Cd^{2+}] concentration

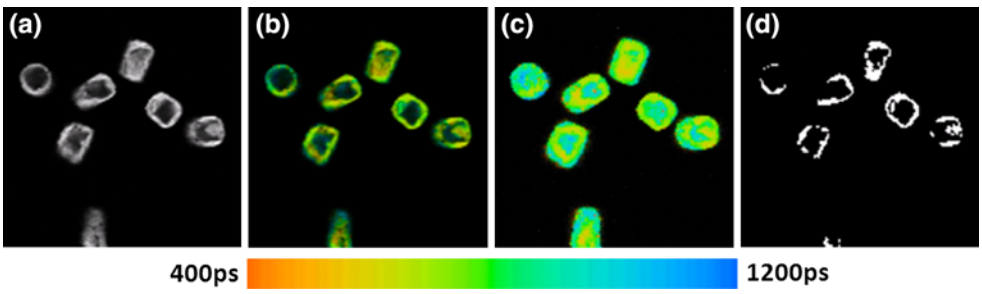

Fig. 1 Image-guided method for the identification of pixels with high signal-to-noise ratio. **a** Intensity-based chlorophyll fluorescence image of *Thalassiosira weissflogii* (excitation power ~400 μw). **b** Corresponding average fluorescence lifetime image. **c** Average fluorescence lifetime image without intensity information. **d** Extracted pixels for statistical analysis

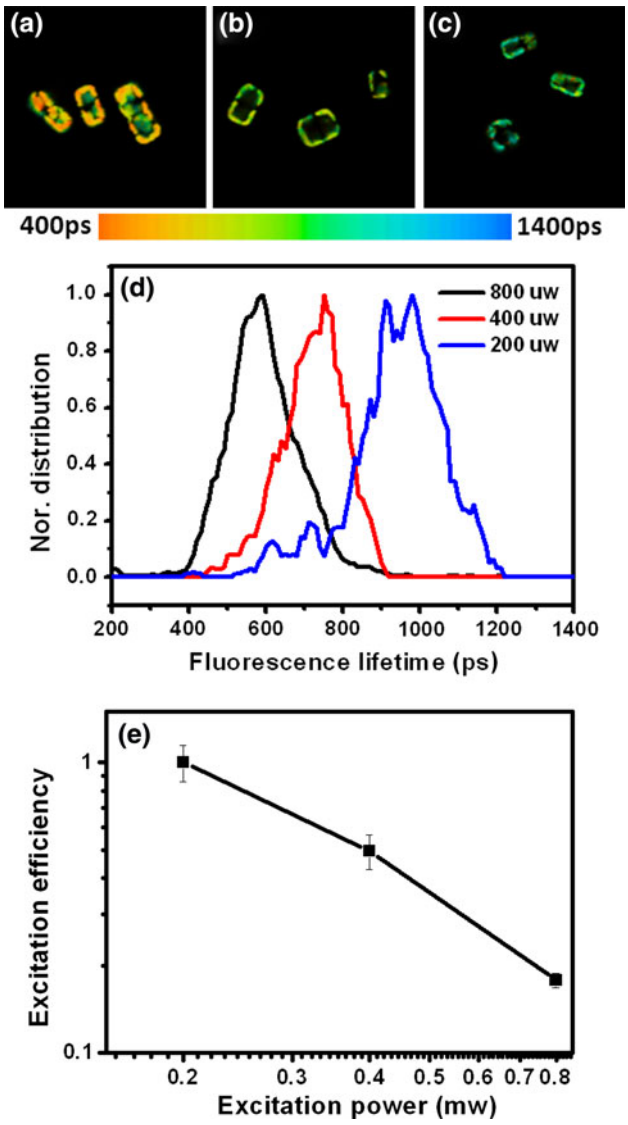

Fig. 2 Characteristics of average fluorescence lifetime images of *Thalassiosira weissflogii* excited at different laser power levels. **a–c** Fluorescence lifetime images of *T. weissflogii* recorded with laser power excitation of 200, 400 and 800 μw, respectively. **d** The average chlorophyll fluorescence lifetime distributions at three excitation power levels. **e** Relative excitation efficiency at different excitation power level

treatment while the chloroplast remained around the vacuole in the other samples. In addition, significant average fluorescence lifetime increase can be directly observed in the sectioning color-coded images (from orange to blue). Quantitatively, the incremental shifts among the distributions of average fluorescence lifetime value extracted from the samples exposed to different concentrations of Cd are shown in Fig. 4h. The peak of fluorescence lifetime distribution shifts from 580 ps for the control samples to 750 ps for the highest [Cd^{2+}] treated ones. These shifts originated from the increases of the two lifetime components as shown in Table 2. The results of statistical analysis in Table 2 also demonstrate the continuous increment trend of the average chlorophyll fluorescence lifetime. The prolongation of the fluorescence lifetime being less at the [Cd^{2+}] concentration of 9.8×10^{-8} M than at 2.5×10^{-8} M may be due to sample variation or statistical aberration. The Student's *T* test indicates that the change of the fluorescence lifetime is at statistically significant level ($P < 0.01$) even with low [Cd^{2+}] concentration (9.67×10^{-11} mol L^{-1})-treated samples. The strong correlation of the temporal characteristics of chlorophyll fluorescence shown in Fig. 4h and Table 2 with the specific growth rates in Fig. 3 clearly indicates that the chlorophyll fluorescence lifetime distribution provides valuable information for in vivo assessment of Cd toxicity. Furthermore, the advantage of TPE-FLIM method is clear because though the commonly used specific growth rate is a noninvasive measurement, it cannot be used for in vivo continuous monitoring of biological processes.

To study the effect of excitation power on the fluorescence decay-based assessment of Cd toxicity, we conducted the FLIM measurements with lower excitation power. The results for the [Cd^{2+}]-treated *T. weissflogii* at the excitation power of 400 μw were displayed in Fig. 5. Similar rising trend of average fluorescence lifetime and fluorescence lifetime components, as well as the morphological change of chloroplast following the increment of [Cd^{2+}] concentrations can be observed in Fig. 5a–h and Table 2. In contrast, the average fluorescence lifetime

Table 1 The statistical result for fluorescence lifetime parameters of different power excited and DCMU-treated *T. weissflogii*

Excitation Power	200 μw	400 μw		800 μw	
Treatment	Control	Control	DCMU	Control	DCMU
A_1 (%)	72.2 ± 23.0	69.3 ± 23.5	64.7 ± 12.9	67.3 ± 11.1	65.7 ± 12.1
τ_1 (ps)	789.3 ± 224.8	662.0 ± 149.3	695.4 ± 177.4	407.3 ± 109.9	549.4 ± 238.4
τ_2 (ps)	1593.9 ± 657.4	1184.1 ± 414.5	1759.4 ± 416.9	1044.4 ± 162.4	1821.1 ± 597.7
$\tau_{Average}$ (ps)	931.4 ± 120.9	784.8 ± 69.0	1053.7 ± 125.8	609.7 ± 101.6	974.5 ± 282.8

The values given in the table are mean ± standard deviation. A_1, τ_1, τ_2 are the lifetime components in the dual exponential decay. $\tau_{Average}$ is the average fluorescence lifetime value. Pixels are sample numbers we use for the statistical analysis using student *T* test

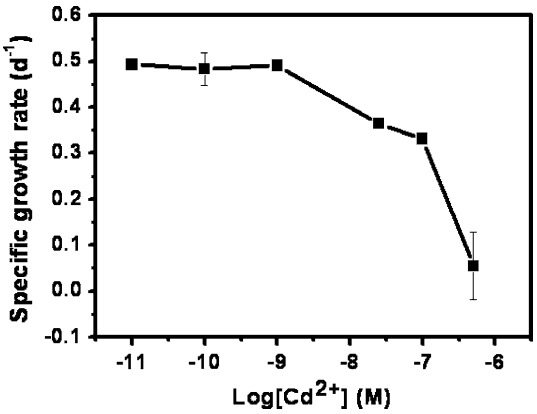

Fig. 3 Specific growth rate of *Thalassiosira weissflogii* treated with different concentrations of [Cd^{2+}] over 72 h. Data are displayed as mean value ± SD for two replicates ($n = 2$)

values were globally higher than that obtained using the higher excitation power. The peak of fluorescence lifetime distribution increases from 780 ps for control samples to 870 ps for the highest [Cd^{2+}] concentration-treated samples. The results are consistent with those obtained using a relatively higher excitation power of 800 μw.

DCMU effect on chlorophyll fluorescence lifetime

DCMU is a well-known electron transport chain inhibitor, which can be utilized to model the changes of chlorophyll fluorescence characteristics during PSII inhibition (Broess et al. 2009; Petrášek et al. 2009). Figure 6a–d shows the average fluorescence lifetime images of the control treatment and the DCMU-treated algal cells. Significant increase of average fluorescence lifetime can be found at both low and high excitation powers. The average fluorescence lifetime value was lower using high excitation power compared with that using lower excitation power. The peaks of fluorescence lifetime distribution (Fig. 6e) were ~580 ps (high power) and ~780 ps (low power) in the control sample, corresponding to 820 ps (high power) and 1,030 ps (low power) in the DCMU-treated samples. The reason for the increase is attributed to the rise of two lifetime components (τ_1, 400 μw excitation: 662–695 ps;

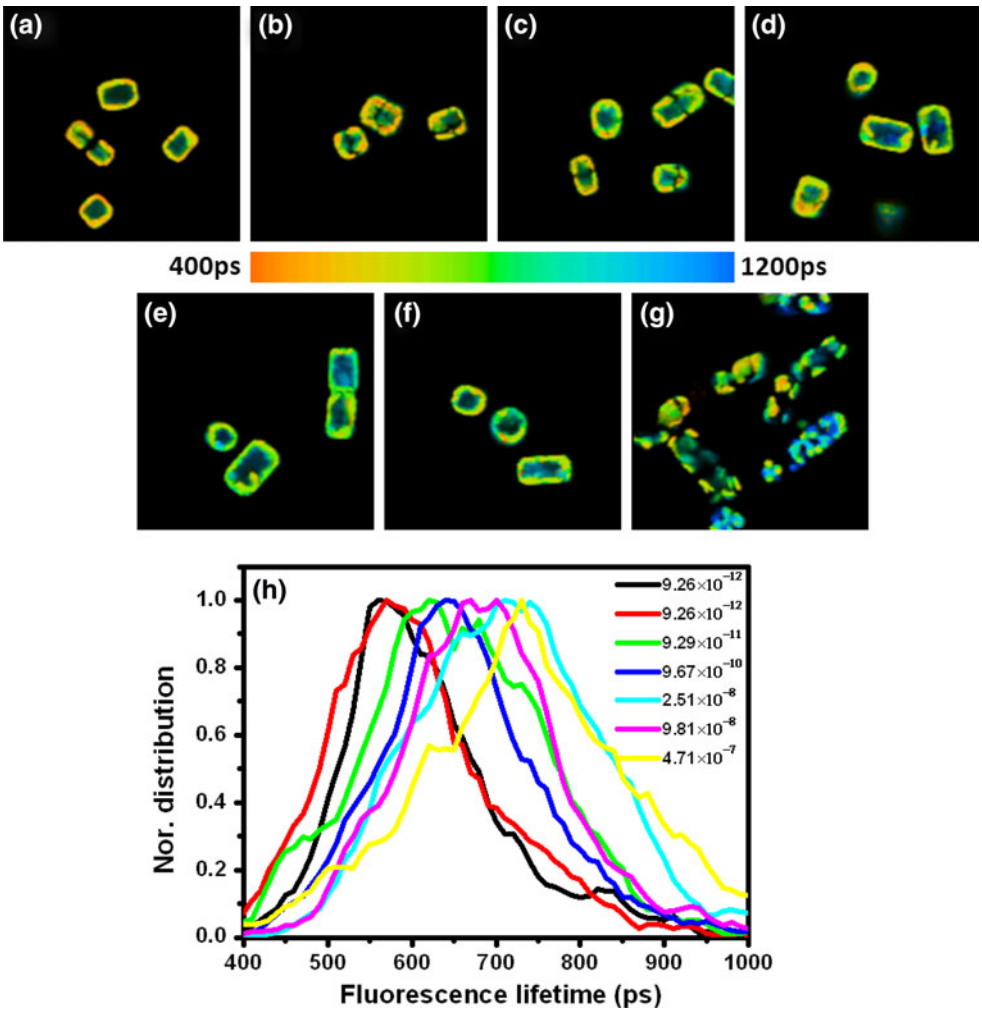

Fig. 4 Characteristics of average fluorescence lifetime images of *Thalassiosira weissflogii* excited by ~800 μw laser power. **a**–**g** Fluorescence lifetime images of *T. weissflogii* under different [Cd^{2+}] concentration treatments at 0 h (**a**) and over 72 h (**b**–**g**) (corresponding to 9.26×10^{-12}, 9.29×10^{-11}, 9.67×10^{-10}, 2.51×10^{-8}, 9.81×10^{-8} and 4.71×10^{-7} mol L^{-1}, respectively). **h** Normalized average chlorophyll fluorescence lifetime distributions

Table 2 The statistical result for fluorescence lifetime parameters of Cd-treated *T. weissflogii*

Excitation power 400 μw							
Cd (mol L^{-1})	9.26×10^{-12}	9.26×10^{-12}	9.67×10^{-11}	9.67×10^{-10}	2.51×10^{-8}	9.81×10^{-8}	4.71×10^{-7}
Time (h)	0	72	72	72	72	72	72
A_1 (%)	69.3 ± 23.5	64.3 ± 18.1	65.6 ± 17.6	63.4 ± 18.3	65.1 ± 17.7	64.5 ± 18.2	66.5 ± 18.0
τ_1 (ps)	662.0 ± 149.3	609.2 ± 127.2	637.0 ± 130.3	648.2 ± 137.0	678.7 ± 142.9	680.2 ± 156.4	692.9 ± 152.8
τ_2 (ps)	1184.1 ± 414.5	1149.7 ± 257.7	1182.8 ± 258.6	1216.4 ± 247.6	1281.2 ± 259.0	1293.6 ± 275	1287.3 ± 298.1
$\tau_{Average}$ (ps)	784.8 ± 69.0	782.4 ± 80.5	805.8 ± 81.7*	836.2 ± 75.6*	871.3 ± 87.5*	879.6 ± 102.5*	869.1 ± 109.47*
Pixels	1,112	2,818	3,404	4,450	3,176	4,196	1,876
Excitation power 800 μw							
Cd (mol L^{-1})	9.26×10^{-12}	9.26×10^{-12}	9.67×10^{-11}	9.67×10^{-10}	2.51×10^{-8}	9.81×10^{-8}	4.71×10^{-7}
Time (h)	0	72	72	72	72	72	72
A_1 (%)	67.3 ± 11.1	63.0 ± 11.7	62.9 ± 14.4	60.4 ± 12.3	61.0 ± 13.8	65.4 ± 13.8	64.5 ± 15.4
τ_1 (ps)	407.3 ± 109.9	385.7 ± 125.5	449.2 ± 151.5	408.1 ± 132.2	464.6 ± 146.4	475.6 ± 108.7	523.6 ± 164.5
τ_2 (ps)	1044.4 ± 162.4	965.0 ± 161.5	1023.5 ± 228.5	1028.7 ± 169.9	1110.4 ± 205.8	1081.3 ± 199.9	1194.2 ± 339.7
$\tau_{Average}$ (ps)	609.7 ± 101.6	595.4 ± 104.8*	650.6 ± 130.0*	649.7 ± 104.3*	708.1 ± 113.5*	674.1 ± 93.2*	746.0 ± 163.2*
Pixels	3,910	3,305	4,515	5,541	5,587	5,143	5,163

The values given in the table are mean ± standard deviation. A_1, τ_1, τ_2 are the lifetime components in the dual exponential decay. $\tau_{Average}$ is the average fluorescence lifetime value. Pixels are sample number we use for the statistical analysis

* Indicates that P value ($P < 0.01$) in the average lifetime using student T test

800 μw excitation: 407–549 ps; τ_2, 400 μw excitation: 1,184–1,759 ps; 800 μw excitation: 1,044–1,821 ps). Table 1 gives the typically statistical presentation of the distributions.

Discussion

High excitation photo density shortened the chlorophyll fluorescence lifetime in *Thalassiosira weissflogii*

A challenge for the application of laser-scanning FLIM in chlorophyll fluorescence study is the high density of excited photons at the focal point causing fluorescence quenching (state transition, singlet–singlet annihilation and proton gradient dependent quenching), leading to the alteration of the fluorescence lifetime (Gilmore et al. 1995; Barzda et al. 2001) and the drop of fluorescence excitation efficiency (Schödel et al. 1996). The shortening of fluorescence lifetime is attributed to the singlet–singlet annihilation and proton gradient-dependent quenching (Gilmore et al. 1995; Barzda et al. 2001) while a slight increase of relative long lifetime amplitude A_2 may be due to the phosphorylation of light-harvesting antenna complex II of PSII (Iwai et al. 2010). The relationships between the chlorophyll fluorescence lifetime as well as the excitation efficiency and the laser excitation power revealed in this study demonstrate that the control of excitation laser power is crucial for chlorophyll fluorescence decay-based assessment. In the Cd toxicity study, we found that the incremental trend of fluorescence lifetime with the treatment of increasing Cd concentrations is the same for the different excitation power levels, though the lifetime distributions are dependent on the excitation power. Therefore, the fluorescence annihilation effect due to high excitation intensity in plants is not an obstacle for applying laser-scanning FLIM as long as the excitation power level is well controlled for all the measurements. However, relative low excitation power is still preferred because of less fluorescence quenching. In addition, the samples of high cell density can be used to further reduce the variation of average fluorescence lifetime distributions.

Cd toxicity led to decrease of algae-specific growth rate and distortion of chloroplast of *Thalassiosira weissflogii*

Cadmium is one of the most toxic metals known to cause ecosystem damage and potentially endanger human health through food train transport. Consistent with the previous results, our study show that the presence of $[Cd^{2+}]$ in the range of 10^{-8} to 10^{-7} M after 72 h of exposure significantly inhibited the growth of *T. weissflogii* (Miao et al. 2005). Compared with the commonly used endpoints (e.g. growth rate, biomass), chlorophyll fluorescence detections have emerged as a more rapid and efficient way to study Cd

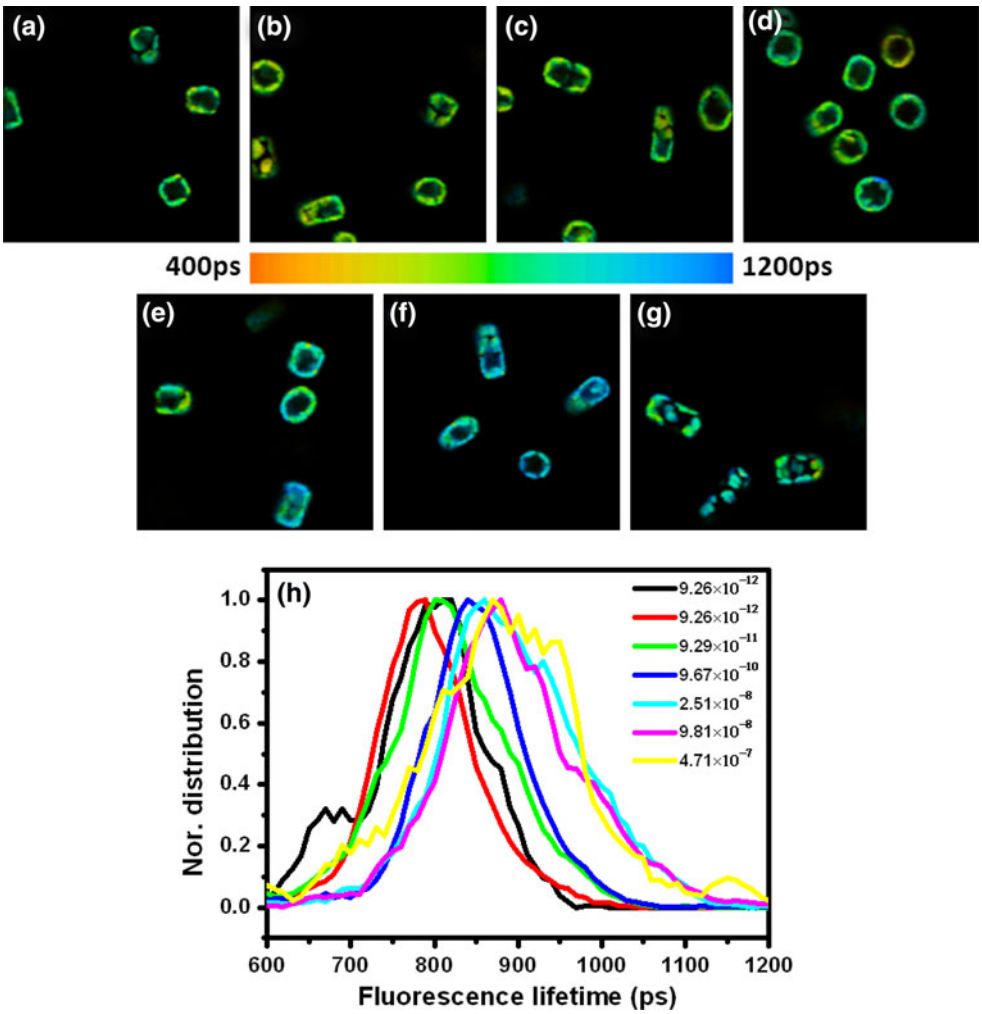

Fig. 5 Characteristics of average fluorescence lifetime images of *Thalassiosira weissflogii* excited by ~400 μw laser power. **a**–**g** Fluorescence lifetime images of *T. weissflogii* under different [Cd^{2+}] concentration treatments at 0 h (**a**) and over 72 h (**b**–**g**) (corresponding to 9.26×10^{-12}, 9.29×10^{-11}, 9.67×10^{-10}, 2.51×10^{-8}, 9.81×10^{-8} and 4.71×10^{-7} mol L^{-1}, respectively). **h** Normalized average chlorophyll fluorescence lifetime distributions

toxicity noninvasively (Maxwell and Johnson 2000; Baker 2008). For example, laser-induced chlorophyll fluorescence spectrum provides the information on the photosynthetic-pigment-content alteration in leaf in vivo (*Cajanus cajan L.*) due to Cd treatment (Maurya and Gopal 2008). PAM has been utilized to quantify the toxic effect of Cd on electron transport chain in the PSII (Miao et al. 2005). In the present study, using two-photon FLIM based on the intrinsic chlorophyll fluorescence, we found that the chlorophyll fluorescence can provide morphological and biochemical information on the chloroplast structures and the status of photosynthesizing activities. The measurement is only physically based and does not require sample preprocessing. Benefitting from the high fluorescence quantum yield of chlorophyll molecule, each fluorescence image is captured within 8 s, achieving the rapid testing. In addition to the fluorescence lifetime measurements, the fluorescence intensity images clearly show serious chloroplast degradation under high [Cd^{2+}] concentration exposure. Although it is difficult to resolve which part of the chloroplast (grana or stroma) was demolished in fine detail under current optical resolution, fragile and irregular chloroplast structures can still be observed. Such degradation may result from functionality alteration of thylakoids by lipid peroxidation (Vassilev et al. 2004), lipoxygenase induction (causing oxidation of polyunsaturated fatty acid) (Somashekaraiah et al. 1992), increased galactolipase activity (leading to hydrolysis of monogalactolipid as well as premature senescence) (Krupa and Baszynski 1995) and disturbances to the chlorophyll biosynthesis (Pandey and Sharma 2002; Stobart et al. 1985). This information could also be used as a biomarker of Cd toxicity. It should be emphasized that TPE fluorescence imaging approach provides three-dimensional spatial resolution and specific structure recognizability for chloroplast. In future study, we will explore how to take the advantage of 3-D imaging capability of TPE-FLIM for the quantification of the degradation and make it as a quantitative indicator of Cd toxicity.

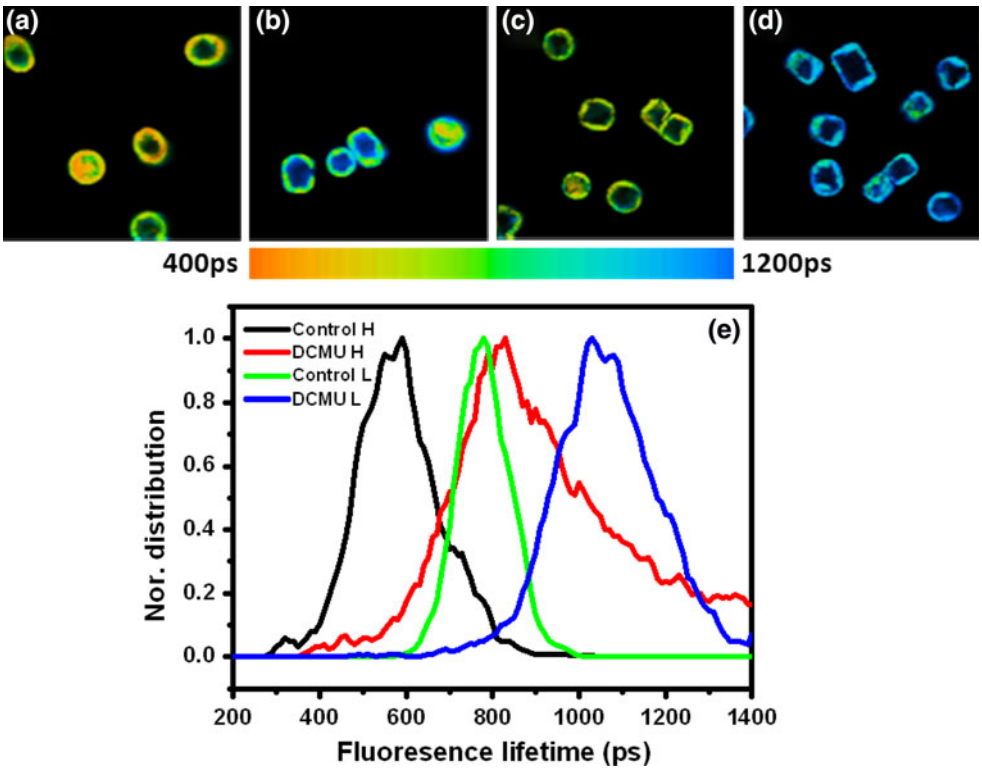

Fig. 6 Characteristics of average fluorescence lifetime images of *Thalassiosira weissflogii* treated with DCMU. **a** Fluorescence lifetime images of *T. weissflogii* in control treatment under high excitation power. **b** Fluorescence lifetime images of *T. weissflogii* in DCMU treated ones under high excitation power. **c** Fluorescence lifetime images of *T. weissflogii* in control treatment under lower excitation power. **d** Fluorescence lifetime images of *T. weissflogii* in DCMU-treated ones under lower excitation power. **e** Normalized average chlorophyll fluorescence lifetime distributions

Cd toxicity led to increment of chlorophyll fluorescence lifetime of *Thalassiosira weissflogii*

Besides the intensity-based chlorophyll fluorescence images, excited state kinetics of fluorescence molecules can be visualized using fluorescence lifetime. In this study, we found increase of the average fluorescence lifetime following increased [Cd^{2+}] concentrations, demonstrating that chlorophyll fluorescence lifetime can be utilized as a new and sensitive biomarker for indicating the toxicity of Cd. It has been shown in Fig. 3 that the major shift of fluorescence lifetime distribution occurs mainly at lower Cd concentration levels, while the specific growth rates drop significantly at higher Cd concentration levels. The results indicate that the specific growth rate is not sensitive to Cd toxicity at relatively low Cd exposure, whereas the fluorescence lifetime distribution has a sensitive response to Cd exposure either in high-power or low-power excitation. The specific growth rate may reflect Cd-toxic effects in not only the photosynthesis system but also in other metabolic processes with higher Cd concentration, while the shift of fluorescence lifetime is probably due to the toxic effect of Cd on electron transport chain in photosynthesis system (Baszynski et al. 1980; Siedlecka and Baszynski 1993; Krupa and Baszynski 1995; Vassilev et al. 2004). Therefore, the specific growth rate and average chlorophyll fluorescence lifetime are complementary parameters to asses Cd toxicity.

DCMU prolongates the chlorophyll fluorescence lifetime by blocking the PSII electron transport chain

It has been reported that oxygen evolving complex (OEC) activities weakened during Cd treatment. This suggests that Cd preferably interacts with the donor side of the PSII leading to inhibition of PSII activities (Vassilev et al. 2004). The PSII reaction center and its redox components are also affected by Cd, influencing PSII electron transport on its way from pheophytin via Q_A and Fe to Q_B (Krupa and Baszynski 1995). The inhibition of electron flow around Photosystem I is due to Cd-induced Fe deficiency (Siedlecka and Baszynski 1993). Moreover, longer fluorescence lifetime decay in *Arabidopsis* leaf was observed when the electron transport chain was blocked by the infiltrated DCMU (Broess et al. 2009). Our study confirms this alteration in the unicellular algae model in vivo. In detail, significant lifetime increase was found after being treated with DCMU. Both lifetime components (τ_1, τ_2) rose, which is consistent with that observed in the Cd-treated algae cells. Furthermore, the shift of lifetime distribution measured from DCMU-treated samples is larger than that in the highest [Cd^{2+}]-treated *T. weissflogii* at both excitation power levels. This is probably attributed to the fact that DCMU almost completely blocks the electron transport (Broess et al. 2009), while the electron transport chain in the Cd-treated algae may be partially blocked.

Conclusions

We demonstrated a rapid and noninvasive method based on the TPE-FLIM for assessing Cd-induced toxicity in algal cells. Average chlorophyll fluorescence lifetime, which was well correlated with the specific growth rate, but more sensitive, can be utilized as a sensitive biomarker for examining Cd toxicity. A Cd-induced increase of average chlorophyll fluorescence lifetime is mainly contributed by the inhibition of the electron transport chain. Such alteration trend was confirmed by utilizing DCMU-treated model. Our recently published results of assessment of Hg toxicity on photosynthesis of *T. weissflogii* (Wu et al. 2012) and the results of this work demonstrate the robustness and applicability of TPE-FLIM as an emerging technology potentially applied for rapid and noninvasive test of heavy metal-induced toxicity. Finally, though the current TPE-FLIM system is still expensive and bulky because of a standard Ti:sapphire femtosecond laser is used as the excitation source, new ultrafast source based on optical fiber laser technology is already commercially available (IMRA fiber laser). This technological advance could tremendously reduce the cost and size of the TPE-FLIM system.

Acknowledgments This work was supported by the Hong Kong Research Grants Council through grants 662711,N_HKUST631/11 and T13-706/11-1, and HKUST through grant RPC10EG33.

References

Baker NR (2008) Chlorophyll fluorescence: a probe of photosynthesis in vivo. Annu Rev Plant Biol 59:89–113

Barzda V, Gulbinas V, Kananavicius R, Cervinskas V, van Amerongen H, van Grondelle R, Valkunas L (2001) Singlet–singlet annihilation kinetics in aggregates and trimers of LHCII. Biophys J 80:2409–2421

Baszynski T, Wajda L, Krol M, Wolinska D, Krupa Z, Tukendorf A (1980) Photosynthetic activities of cadmium-treated tomato plants. Physiol Plant 48:365–370

Bertrand M, Poirier I (2005) Photosynthetic organisms and excess of metals. Photosynthetica 43:345–353

Broess K, Borst JW, van Amerongen H (2009) Applying two-photon excitation fluorescence lifetime imaging microscopy to study photosynthesis in plant leaves. Photosynth Res 100:89–96

Das P, Samantaray S, Rout GR (1997) Studies on cadmium toxicity in plants: a review. Environ Pollut 98:29–36

ElJay A, Ducruet JM, Duval JC, Pelletier JP (1997) A high-sensitivity chlorophyll fluorescence assay for monitoring herbicide inhibition of photosystem II in the chlorophyte *Selenastrum capricornutum*: comparison with effect on cell growth. Arch Hydrobiol 140:273–286

Gilmore AM, Hazlett TL, Govindjee (1995) Xanthophyll cycle-dependent quenching of photosystem II *chlorophyll a* fluorescence: formation of a quenching complex with a short fluorescence lifetime. Proc Natl Acad Sci USA 92:2273–2277

Hasan SA, Fariduddin Q, Ali B, Hayat S, Ahmad A (2009) Cadmium: toxicity and tolerance in plants. J Environ Biol 30:165–174

Iwai M, Yokono M, Inada N, Minagawa J (2010) Live-cell imaging of photosystem II antenna dissociation during state transitions. Proc Natl Acad Sci USA 107:2337–2342

Juneau P, El Berdey A, Popovic R (2002) PAM fluorometry in the determination of the sensitivity of *Chlorella vulgaris*, *Selenastrum capricornutum*, and *Chlamydomonas reinhardtii* to copper. Arch Environ Contam Toxicol 42:155–164

Krupa Z (1988) Cadmium-induced changes in the composition and structure of the light-harvesting *chlorophyll a/b* protein complex-II in radish cotyledons. Physiol Plant 73:518–524

Krupa Z, Baszynski T (1995) Some aspects of heavy metals toxicity towards photosynthetic apparatus—direct and indirect effects on light and dark reactions. Acta Physiol Plant 7:55–64

Li D, Zheng W, Qu JY (2008) Time-resolved spectroscopic imaging reveals the fundamentals of cellular NADH fluorescence. Opt Lett 33:2365–2367

Maurya R, Gopal R (2008) Laser-induced fluorescence ratios of *Cajanus cajan* L. under the stress of cadmium and its correlation with pigment content and pigment ratios. Appl Spectrosc 62:433–438

Maxwell K, Johnson G (2000) Chlorophyll fluorescence—a practical guide. J Exp Bot 51:659–668

Miao AJ, Wang WX, Juneau P (2005) Comparison of Cd, Cu, and Zn toxic effects on four marine phytoplankton by pulse-amplitude-modulated fluorometry. Environ Toxicol Chem 24:2603–2611

Pandey N, Sharma CP (2002) Effect of heavy metals CO^{2+}, Ni^{2+} and Cd^{2+} on growth and metabolism of cabbage. Plant Sci 163:753–758

Petrášek Z, Schmitt FJ, Theiss C, Huyer J, Chen M, Larkum A, Eichler HJ, Kemnitz K, Eckert HJ (2005) Excitation energy transfer from phycobiliprotein to chlorophyll *d* in intact cells of *Acaryochloris marina* studied by time- and wavelength-resolved fluorescence spectroscopy. Photochem Photobiol Sci 4:1016–1022

Petrášek Z, Eckert HJ, Kemnitz K (2009) Wide-field photon counting fluorescence lifetime imaging microscopy: application to photosynthesizing systems. Photosynth Res 102:157–168

Schödel R, Hillmann F, Schrötter T, Voigt J, Irrgang KD, Renger G (1996) Kinetics of excited states of pigment clusters in solubilized light—harvesting complex II: photon density-dependent fluorescence yield and transmittance. Biophys J 71:3370–3380

Siedlecka A, Baszynski T (1993) Inhibition of electron flow around photosystem-I in chloroplasts of Cd-treated maize plants is due to Cd-induced iron-deficiency. Physiol Plant 87:199–202

Somashekaraiah BV, Padmaja K, Prasad ARK (1992) Phytotoxicity of cadmium ions on germinating seedlings of mung bean (*Phaseolus vulgaris*)—involvement of lipid peroxides in chlorophyll degradation. Physiol Plant 85:85–89

Stobart AK, Griffiths WT, Ameenbukhari I, Sherwood RP (1985) The Effect of Cd^{-2+}on the biosynthesis of chlorophyll in leaves of barley. Physiol Plant 63:293–298

Szabó I, Bergantino E, Giacometti GM (2005) Light and oxygenic photosynthesis: energy dissipation as a protection mechanism against photo-oxidation. EMBO Rep 6:629–634

Tirlapur UK, König K (2001) Femtosecond near-infrared lasers as a novel tool for non-invasive real-time high-resolution time-lapse imaging of chloroplast division in living bundle sheath cells of Arabidopsis. Planta 214:1–10

Tkalec M, Prebeg T, Roje V, Pevalek-Kozlina B, Ljubesic N (2008) Cadmium-induced responses in duckweed *Lemna minor* L. Acta Physiol Plant 30:881–890

Trampe E, Kolbowski J, Schreiber U, Kuhl M (2011) Rapid assessment of different oxygenic phototrophs and single-cell photosynthesis with multicolour variable chlorophyll fluorescence imaging. Mar Biol 158:1667–1675

Vassilev A, Lidon F, Scotti P, Da Graca M, Yordanov I (2004) Cadmium-induced changes in chloroplast lipids and photosystem activities in barley plants. Biol Plant 48:153–156

Wu Y, Zeng Y, Qu JY, Wang WX (2012) Mercury effects on *Thalassiosira weissflogii*: applications of two-photon excitation chlorophyll fluorescence lifetime imaging and flow cytometry. Aquat Toxicol 110–111:133–140

Zeng Y, Jiang L, Zheng W, Li D, Yao S, Qu JY (2011) Quantitative imaging of mixing dynamics in microfluidic droplets using two-photon fluorescence lifetime imaging. Opt Lett 36:2236–2238